# Accounting for data uncertainty in modeling acute respiratory infections: influenza in Saint Petersburg as a case study *

Kseniya Sahatova, Aleksandr Kharlunin, Israel Huaman[0000−0003−4677−8259], and Vasiliy Leonenko[0000−0001−7070−6584]

ITMO University, 49 Kronverksky Pr., St. Petersburg, Russia 197101

**Abstract.** Epidemics of acute respiratory infections, such as influenza and COVID-19, pose a serious threat to public health. To control the spread of infections, statistical methods and mathematical models are often used to estimate and forecast epidemic indicators. The assessment of values of these indicators might be impacted by the uncertainty in the initial data used for model calibration. The dependence of modeling results on accuracy of the data can be huge, and the lack of its consideration, which is typical for most works on modeling the spread of epidemic ARIs, makes it difficult to correctly predict the effectiveness of anti-epidemic measures. In this research, we present methods and algorithms for uncertainty estimation in retrospective analysis and forecasting of the incidence of epidemic ARIs. The uncertainty assessment is performed by replicating simulated incidence curves with assumed random errors which distribution is defined by the variance of the original incidence dataset. The application of the methods is demonstrated on an example, with influenza outbreak in St. Petersburg, Russia, as a case study.

**Keywords:** mathematical modeling · epidemiology · influenza · data uncertainty

## 1 Introduction

Epidemics of acute respiratory viral infections, with influenza and COVID-19 being the leading ones, pose a serious threat to public health and the economic development of the affected countries [13]. To contain the epidemic spread, health authorities use comprehensive measures, such as quarantine and vaccination. To provide adequate justification to the planned interventions, health organs often rely on statistical and mechanistic models calibrated to disease incidence data. One of the most popular approaches is connected with so called compartmental models. Compartmental models have been a powerful tool in mathematical modeling of epidemiological processes for many years. During the COVID-19

* This research was supported by The Russian Science Foundation, Agreement #22-71-10067

ICCS Camera Ready Version 2023
To cite this paper please use the final published version:
DOI: 10.1007/978-3-031-36024-4_23

they were actively used to predict the evolution of the pandemic and to estimate the effect of health interventions. Comparing to the prediction and decision support systems based on machine learning methods, such as deep neural networks, the output of the compartmental models is much easier to interpret. Using interpretable models is beneficial for decision makers compared to 'black box' approaches, which contributes to the popularity of classical mechanistic models in analysing epidemic dynamics. A comparison of the strengths and weaknesses of the mentioned approaches can be found in [21].

Modeling of epidemiological processes is often a challenging task, considering the fact that the epidemiological data is prone to errors. As a consequence, the modeling output might not properly represent the real situation, which leads to subpar policies in epidemic containment. It is crucial to employ the systems that consider and unite all potential sources of uncertainty to increase the trust to decisions made on their basis. Main difficulties that can cause a misleading prognosis by the models are described in [27]. Since one of the main components of the modeling framework is input data, its quality and quantity influences the uncertainty in the output of the model.

The aim of this work is to characterize uncertainty in ARI incidence data, estimate the confidence intervals for model parameters and assess the corresponding variation in disease dynamics forecasts. For this purpose, we use an influenza epidemic model employed in our earlier research [8]. This model is described in detail in Section 2. Section 3 provides a description of experiments for parameter uncertainty estimation using the computational approach presented by Chowell et al [3]. The results are discussed in Section 4.

## 2 Methods

### 2.1 Incidence data

The dataset used in the study was based on the data provided by the Research Institute of Influenza. By combining ARI incidence data in 2010–2011 for Saint Petersburg, Russia, and the results of virological testing performed during the same season, we found the numbers for weekly clinically registered cases of ARI attributed to different influenza strains [15]. Although in this research only one season was used in the experiments, the described algorithm is versatile enough to be applied to any other epidemic season in a given Russian city which has sufficient volume of reported incidence and virological testing.

### 2.2 Modeling framework

The epidemic model used in this study is a SEIR–type discrete compartmental model represented by a system of difference equations. This model has a flexible structure which allows to distinguish infections caused by different influenza strains [15] and track them separately in different age groups [14]. In this paper, we use the simplest version of the model structure, in which we do not regard

ICCS Camera Ready Version 2023
To cite this paper please use the final published version:
DOI: 10.1007/978-3-031-36024-4_23

age groups and specific strains. The following system of equations is used in the model:

$$x_{t+1}^{(h)} = \max\left\{0, \left(1 - a\frac{\beta}{\rho}\overline{y}_t\right) x_t^{(h)}\right\}, h \in \overline{1,2},$$
$$y_{t+1} = \frac{\beta}{\rho}\overline{y}_t \sum_{h=1}^{n_s+1} a x_t^{(h)},$$
$$\overline{y}_t = \sum_{\tau=0}^{T} y_{t-\tau} g_\tau,$$
$$x_0^{(h)} = \alpha^{(h)}((1-\mu)\rho - y_0) \geq 0, h \in \overline{1,2},$$
$$y_0 = \varphi_0 \geq 0.$$

where $x_{t+1}^{(h)}$ corresponds to the fraction of susceptible individuals at the time moment $t+1$ with exposure history $h \in \overline{1,2}$, $y_{t+1}$ corresponds to the amount of newly infected individuals at the time moment $t+1$, $\overline{y_t}$ corresponds to the total amount of infected by the time $t$. A group $x_t^{(1)}$ of susceptible individuals with exposure history state $h = 1$ is composed of those individuals who were subjected to infection in the previous epidemic season, whereas a group $x_t^{(2)}$ with exposure history state $h = 2$ is regarded as naive to the infection. The parameter $\alpha^{(h)}$ is a fraction of population exposed to the infection in the preceding epidemic season, $h \in \overline{1,2}$. The variable $\mu \in [0;1)$ reflects the fraction of population which do not participate in infection transmission. The piece-wise constant function $g_\tau$ reflects the change in individual infectiousness over time from the moment of infection. The parameter $\beta$ is the intensity of effective contacts, $\rho$ is the population size. Due to immunity waning, the individuals with the history of exposure to influenza virus in the preceding season might lose immunity in the following epidemic season. We assume that the fraction $a$ of those individuals, $a \in (0;1)$, becomes susceptible, whereas $1-a$ individuals retain their immunity by the moment of the modeled epidemic. We also assume that $\alpha^{(1)} = 1-\alpha^{(2)} = \alpha$, with the proportion $\alpha$ of people exposed to our generic influenza virus strain being a free parameter. More details about the model can be found in [8].

### 2.3 Calibration algorithm

Model calibration procedure consists in finding parameter values which deliver the optimum for the optimization function (1). In this function, weighted sum of squared residuals is minimized. The residuals are calculated as the difference between the incidence data ($Z^{(\mathrm{dat})}$) and the simulated incidence values ($Z^{(\mathrm{mod})}$) for each week. In the previous studies [16], we estimated a plausible range for the epidemiological parameters, which is given in Table 1.

$$F\left(Z^{(\mathrm{mod})}, Z^{(\mathrm{dat})}\right) = \sum_{i=0}^{t_1} w_i \cdot \left(z_i^{(\mathrm{mod})} - z_i^{(\mathrm{dat})}\right)^2 \longrightarrow \min \quad (1)$$

ICCS Camera Ready Version 2023
To cite this paper please use the final published version:
DOI: 10.1007/978-3-031-36024-4_23

Table 1: Estimated epidemiological parameters for model fitting

| Definition | Description | Value range |
|---|---|---|
| $\alpha$ | Individuals with the history of exposure in the previous season | (0.005, 0.9) |
| $\beta$ | Intensity of infectious contacts | (0.03, 0.24) |
| $a$ | Fraction of previously exposed individuals who will lose immunity in the following epidemic season | (0.0, 1.0) |
| $\mu$ | Fraction of population which do not participate in the infection transmission | 0.9 |

The weights $w_i$ included in the formula (1) are used to reflect the 'importance' of fitting the model curve to the particular data points. In case of seasonal influenza, the data closer to the peak have higher plausibility, because the laboratory sample sizes tend to become bigger during a full-fledged outbreak and thus the proportion of different virus strains in the overall ARI incidence is calculated more precisely. Thus, for weight estimation we use the formula $w_i = \sigma^{-d}$, where $d$ is the distance of the current data point from the peak in time units (weeks), $\sigma$ is a parameter related to decreasing rate with growing distance from the peak. More details on model calibration could be found in [14].

The time step of the model is one day, whereas the incidence data has a time step of one week, so to be able to compare the incidences we derive simulated weekly incidence by summing and interpolating the obtained daily values.

To align the simulation timeline $t = 0, 1, \ldots$ with the dates of the epidemic dataset, we assume that the maximum weekly incidence should be attributed to the same time moment in real and simulated data, which gives us a reference point for matching in time the model with data.

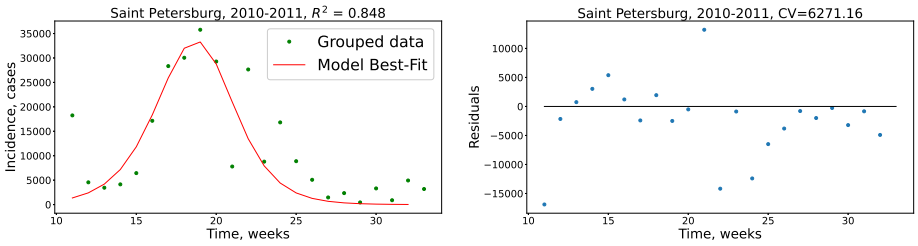


(a) Model best-fit (b) Residuals from model best-fit

Fig. 1: (a) The model calibration to incidence data of the single epidemic season of ARI in St. Petersburg, Russia. Green circles represent the reported weekly case incidence, red line shows the model trajectory, $R^2$ stands for the coefficient of determination. (b) The plot of residuals, CV stands for the coefficient of variation.

ICCS Camera Ready Version 2023
To cite this paper please use the final published version:
DOI: 10.1007/978-3-031-36024-4_23

Figure 1 displays the obtained model best fit. The pattern of the residuals justifies that our model offers a fairly adequate match for the epidemic data.

### 2.4 Forecasting

In addition to the epidemic indicators that are assessed by retrospective analysis of the full incidence dataset, we aim to assess the forecasting uncertainty. The prediction algorithm is based on model calibration on incomplete data which was implemented by the authors in earlier research [17]. In the present study, we modified the prediction algorithm to make it suitable for the current model, and added a new method of aligning in time the simulated curve with the incidence dataset.

In overall, the calibration algorithm on incomplete data which produces a prediction curve does not differ much from the procedure of calibration on complete data. The only difference is in the fact that we do not know a day of the maximum incidence which we used to align the model time frame with real time. To solve this issue, two types of prediction algorithms were proposed with distinct alignment procedures:

- **Primary algorithm**, in which we loop through possible time moments of maximum incidence $t_n$ to $t_{n+k}$, where $t_n$ is the last known incidence from the incomplete dataset and $k = const$ is a calibration parameter. During each iteration, we assume that the regarded point $t_{n+i}$ is the time moment of maximum incidence and we perform the model calibration based on that assumption. As a result, instead of one calibration run in case of the complete dataset we have to perform $k$ calibrations. In the end, we compare the obtained $k$ values of function (1) and select the parameter values which deliver the optimum for (1).
- **Auxiliary algorithm**, in which we assume that the time moment $t = 0$ corresponds to the first date of the incidence dataset, thus we replace the alignment by peak with the alignment by the first day of the epidemic. In general case, due to the uncertainty in detection of the influenza epidemic onset in the ARI dataset [17], it is hardly possible to establish the starting date in an incidence dataset with certainty, so the auxiliary algorithm cannot be employed. At the same time, this algorithm is suitable in case of COVID-19 outbreaks when the starting moment of each wave is more or less defined, and, as it will be discussed later, for making predictions on bootstrapped data. Since for any incidence dataset the first day may be clearly defined, there is no need in looping through possible time alignment alternatives (i.e. only one calibration run is needed), which makes the auxiliary algorithm much faster compared to the primary algorithm. The described algorithm might be also used without changes for the model calibration on complete data (i.e for the retrospective analysis).

ICCS Camera Ready Version 2023
To cite this paper please use the final published version:
DOI: 10.1007/978-3-031-36024-4_23

### 2.5 Uncertainty quantification

**Sources of uncertainty.** Uncertainty in epidemiological data is an important factor to consider since it plays one of the key roles [9] in accuracy of the modeling output along with the structural complexity of models employed [8]. Error measurement in epidemic studies stays one of the main problems of mathematical epidemiology [23]. In [27], the authors highlight the major sources of uncertainty such as a lack of knowledge, biased data, measurement errors, stochasticity of the process, parameter uncertainty, redundant complexity and erroneous structure of the utilized model. Among the sources of uncertainty related in particular to input data, the following ones could be distinguished:

- Noise in incidence data;
- Bias caused by missed historic records during national holidays, scarce data;
- Under-reported cases at the time of weekends;
- Implausible data, which is not reflecting the trend of the epidemic;
- Confounding factors that can or cannot be measured.

The complexity of combination of these factors makes it difficult to estimate the resulting error structure. Thus synthetic error structure models are often used based on known probabilistic distributions.

**Relevant research.** There are various ways to perceive and interpret the uncertainty of the model parameters related to the input data. Valero and Morillas [20] used the bootstrap method based on resampling of incidence data, relying on the fact that they have the greatest influence on the uncertainty of modeling process. Another method is parametric bootstrapping approach from the best-fit model solution proposed by Chowell [24]. This method was successfully used in a handful of studies [4, 19] to characterize the uncertainty of model parameters. The paper [1] identifies the problem of characterization of uncertainty to improve decision making procedures in risk assessments. There is a plethora of research such as [1, 27, 28] that discuss the necessity to consider the corruption of data or the potential bias in it during the assessment of an epidemic indicators. However, not all of these studies provide quantification of this impact on the modeling results. Lloyd [18] and Samsuzzoha et al [26] performed uncertainty analysis of the basic reproduction number with various mathematical and statistical methods. Chowell [3] discusses methods of parameter uncertainty quantification in dynamic models, as well as evaluation of confidence intervals. In paper [11] Krivorot'ko et al. formulated an inverse problem of refining the model parameters and studied the reliability of forecasts by the epidemic models based on the COVID-19 incidence. For the purpose of our research, we selected a method of uncertainty quantification from [3], which is used further in the study.

**Modeling uncertainty.** Our main objective in modeling uncertainty is to select and test particular error structures, which are compatible with incidence data and allow us to encapsulate the sources of uncertainty mentioned earlier.

ICCS Camera Ready Version 2023
To cite this paper please use the final published version:
DOI: 10.1007/978-3-031-36024-4_23

To model the uncertainty of the input data, the Poisson error structure may be used, as it is one of the most popular error models. The modeling framework described by Chowell [2], [3] introduces a bias via generating a random value with Poisson distribution with the mean equal to the number of new registered infection cases in a fixed time step. In our case, we applied the given distribution to weekly incidence dataset. Figure 2 illustrates the variance of simulated residuals acquired after $n = 5000$ resamples on the initial dataset. The empirical distribution demonstrates that the simulated uncertainty is higher on the epidemic peak, while sample values attributed to low incidence (the beginning and the end of the epidemic wave) do not show much variability.

Another approach, which is negative binomial error structure [12], can be used to model higher variance levels in the data as in this case the mean and variance could be set independently, based on the variability of residuals. It can be useful for disease modeling in situations, where distributions with overdispersion provide better representation of the actual data [25]. Taking the epidemic data overdispersion into account in simulation is often crucial, considering that in practical situations, especially in sparse time series, variance can be much larger than the mean and this fact should not be ignored [10]. For cases of excessive data variability we used error structure based on zero-truncated negative binomial distribution [7] to exclude zeros that were not eliminated in the data correction process.

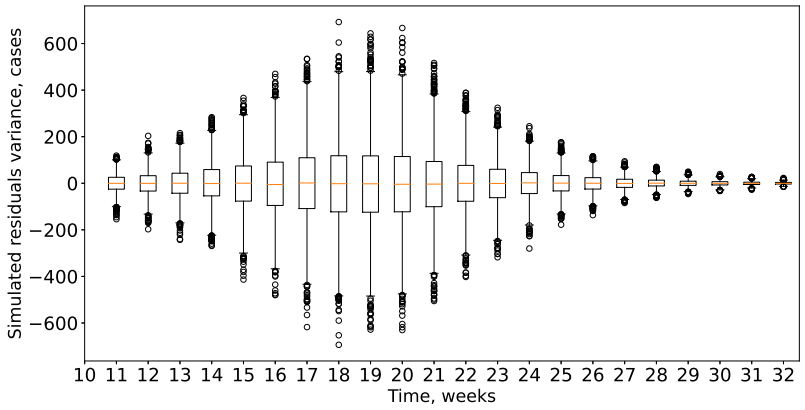


Fig. 2: The empirical distribution of residuals obtained using Poisson error structure

ICCS Camera Ready Version 2023
To cite this paper please use the final published version:
DOI: 10.1007/978-3-031-36024-4_23

## 3 Experiments and results

### 3.1 Interval estimates of model parameters

To actually perform the estimation of the parameter uncertainty, we use the parametric bootstrap method [6] based on best-fit model curve resampling [5]. Such choice allows us to take into account different approaches to treating parameter uncertainty. The implemented algorithm has the following steps:

- Obtain the best-fit parameter values $\hat{\theta} = (\hat{\alpha}, \hat{\beta}, \hat{a})$ for simulated incidence $Z_1^{(\text{mod})}(\hat{\theta})$ and corresponding residuals $\rho_i = z_i^{(\text{mod})}(\hat{\theta}) - z_i^{(\text{dat})}$ by calibrating the model to the original incidence data incidence.
- Generate $m = 200$ datasets $Z_1^{'(\text{dat})}, ..., Z_{200}^{'(\text{dat})}$ based on $Z^{(\text{mod})}(\hat{\theta})$ incidence curve with the addition of generated residuals: $z_i^{'(\text{dat})} = z_i^{(\text{mod})}(\hat{\theta}) + \delta_i$ In the first set of experiments, to determine the residual value $\delta_i$ at time $t_i$ we used Poisson distribution function $\delta_i \sim Pois(\lambda(t_i))$ in which $\lambda(t_i) = z_i^{(\text{mod})}(\hat{\theta})$ [2]. In the second set of experiments, the assumed error structure was based on zero-truncated negative binomial distribution. In the latter case, the residual values $\delta_i$ have a distribution $\delta_i \sim NB(r, p)$ with parameters $r$ and $p$ defined so that the expressions $\mu = z_i^{(\text{mod})}(\hat{\theta})$ and $\sigma^2 = \nu$ hold true. The value $\nu$ was derived experimentally due to the fact that there is no generally accepted form for calculating the variance for the simulated error structure, given that it must cover the potential error spread in the incidence data. As a result of empirical observations, the variance of the error is considered equal to the standard deviation of residual sample $\rho$, i.e. $\nu = \sigma_\rho$.
- Re-estimate the model parameters by calibrating the model on the generated data $Z_1^{'(\text{dat})}, ..., Z_{200}^{'(\text{dat})}$. At this step we assume that the initial day of an epidemic is clearly defined (it was essentially established during the previous steps when the model was calibrated to original data), thus, the calibration procedure might be performed by means of an auxiliary algorithm (matching by initial day of the epidemic).
- Characterise the distribution of model parameters. $\theta_1^*, ..., \theta_m^*$ The percentile method [22] was used to obtain confidence intervals.

The described approach allows flexibility in choosing the error structure, which is its advantage. The computational experiments revealed the major drawback of this method, which is its computational complexity [3]. However, the usefulness of this technique exceeds its limitations, which justified its recurrent usage in various studies [4, 19]

Figure 3 demonstrates a set of curves compared to the initial model in bootstrap procedure, while Figure 4 and Table 2 show results of the uncertainty estimation for epidemiological parameters, with total number of the infected chosen as an example.

ICCS Camera Ready Version 2023
To cite this paper please use the final published version:
DOI: 10.1007/978-3-031-36024-4_23

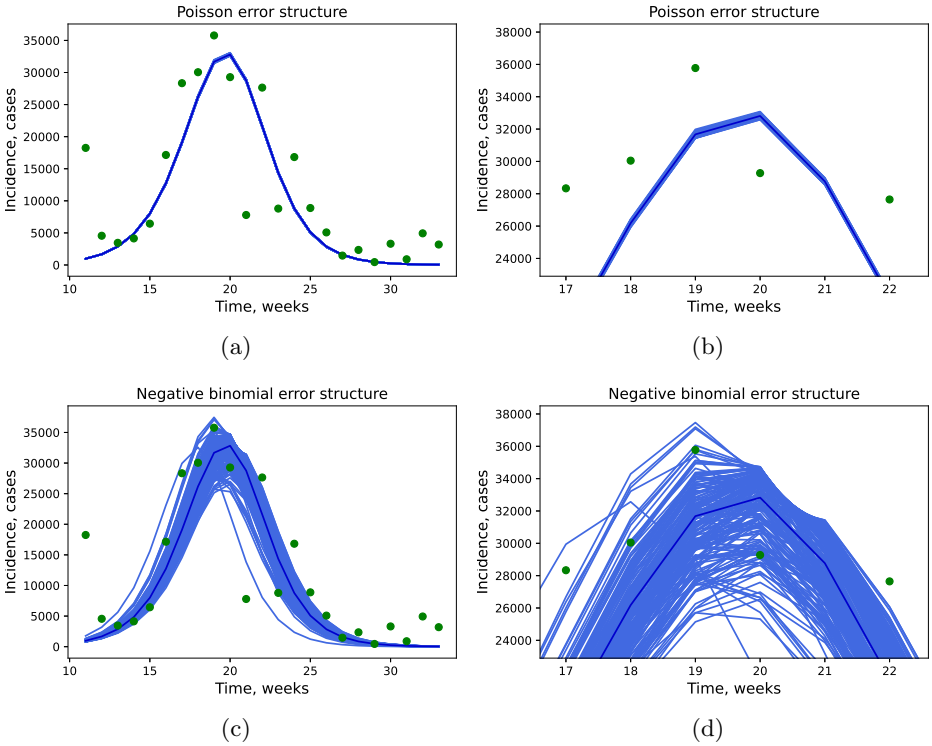


Fig. 3: Visualization of re-fitted curves after bootstrap procedure for the epidemic season of ARI at 2010-2011 in St. Petersburg, Russia, for Poisson (a,b) and negative binomial (c,d) error structures

## 4 Model forecast

In this section, we demonstrate how the uncertainty quantification approach can be applied for interval forecasting. In this case, the bootstrapped datasets are generated in the same way as it was described earlier, i.e. based on the simulated modeling curve. The simulated incidence values for each week were used as mean values of the bias with Poisson and negative binomial distributions. Lower incidence values produce narrower distribution of the synthetic data points around the mean, and vice versa. As it is demonstrated in Fig. 5, the sample distribution of 200 bootstrapped incidence values with Poisson error for $15^{\text{th}}$ week is wider than those distributions for $25^{\text{th}}$ and $10^{\text{th}}$ weeks, because it is closer in time to the peak of the outbreak.

During the prediction procedure, we use the calibration algorithms described in Section 2.4. The first step includes the calibration based on iterative alignment of the epidemiological peak (primary algorithm). During the resampling procedure, an auxiliary algorithm is used to calibrate the model to the boot-

ICCS Camera Ready Version 2023
To cite this paper please use the final published version:
DOI: 10.1007/978-3-031-36024-4_23

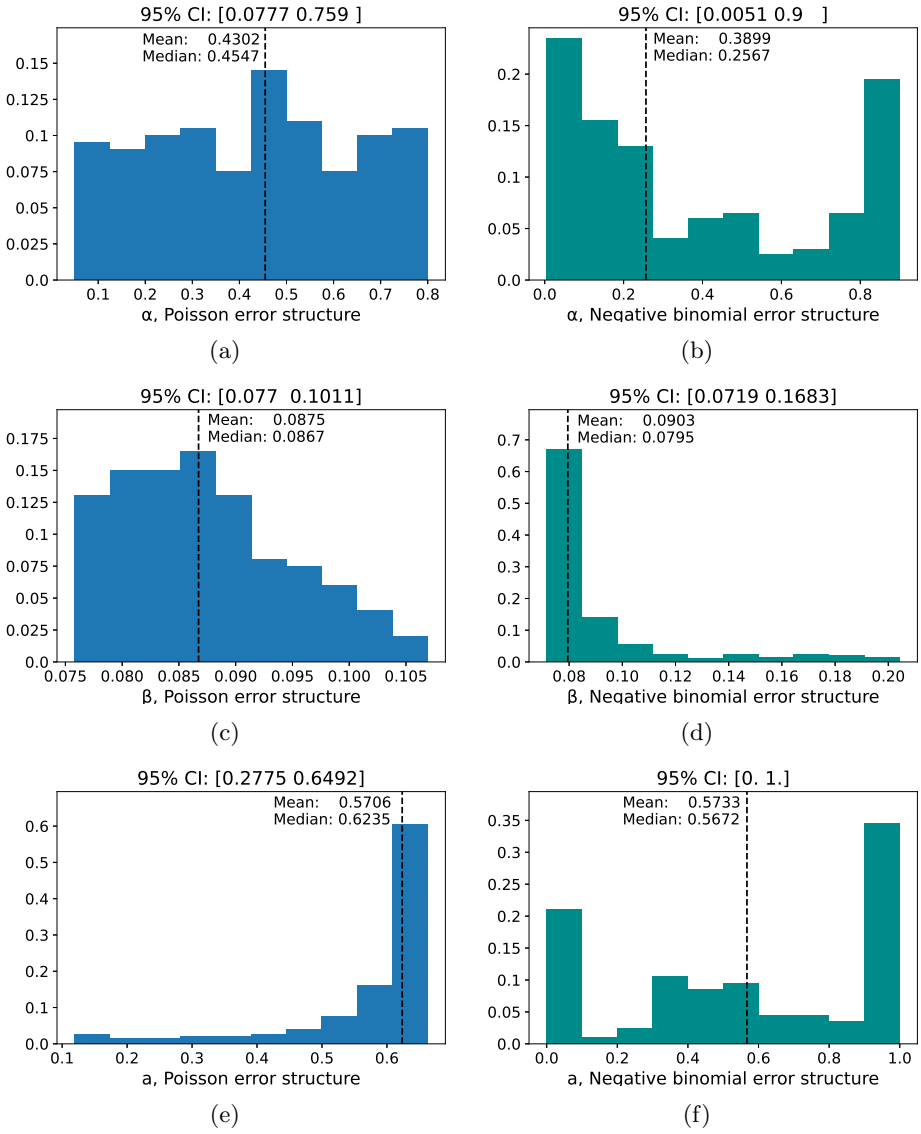


Fig. 4: The empirical distributions for parameter estimations after re-fitting of parameters to the single epidemic season with different error structures. Dashed vertical line represents the median of given parameter.

ICCS Camera Ready Version 2023
To cite this paper please use the final published version:
DOI: 10.1007/978-3-031-36024-4_23

Table 2: Interval estimates for epidemic indicators and fit quality

| Parameter | Poisson | | Negative binomial | |
|---|---|---|---|---|
| | Mean | 95% CI | Mean | 95% CI |
| Total recovered | 226948.79 | (226091.13, 227849.43) | 223786.87 | (201687.25, 238776.42) |
| $R^2$ | 0.99997 | (0.99994, 0.99999) | 0.9576 | (0.9116, 0.9842) |

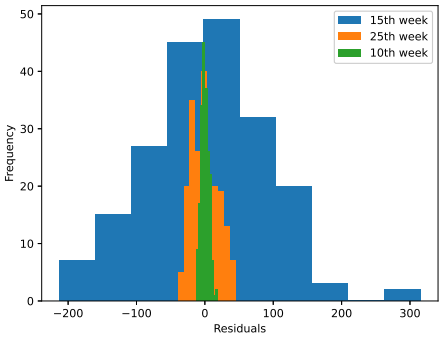


Fig. 5: The simulated residuals empirical distribution obtained using Poisson error structure visualised on the given outbreak

strapped incidence curves. Figure 6 shows a result of the forecasting procedure. The prediction was performed on the data samples comprised of first 5 and 7 data points after the outbreak inception. The grey curves show the variability of the forecast. A bunch of curves which correspond to simulated datasets with Poisson error distribution (Figure 6a, 6c) is quite narrow which does not correspond to the distribution of incidence data. Thus, it could be assumed that there are some sources of uncertainty introducing overdispersion into the data that should be modeled by some other distribution — for instance, negative binomial distribution. In fact, the bootstrapped curves with the bias generated according to negative binomial distribution provided coverage of the most data points, which may be seen in Figures 6b, 6d. Figure 6 also demonstrates that the width of the obtained set of curves depends on the size of data sample used for the calibration. The less amount of data is used, the wider a bunch of the bootstrapped curves is, which is notable in figures 6b and 6d. The quality metric used for evaluating the forecast quality is the root mean squared errors (RMSE):

$$RMSE(\mathbf{y}, \hat{\mathbf{y}}) = \sqrt{\frac{1}{n}\sum_{i=1}^{n}(y_i - \hat{y}_i)^2}.$$

This value is calculated for every prediction curve, thus forming a sample. The means and CI for the samples of RMSE values are provided in Table 2 for the

ICCS Camera Ready Version 2023
To cite this paper please use the final published version:
DOI: 10.1007/978-3-031-36024-4_23

forecasts made with 5, 6, and 7 initial data points and two error distributions (Poisson and negative binomial).

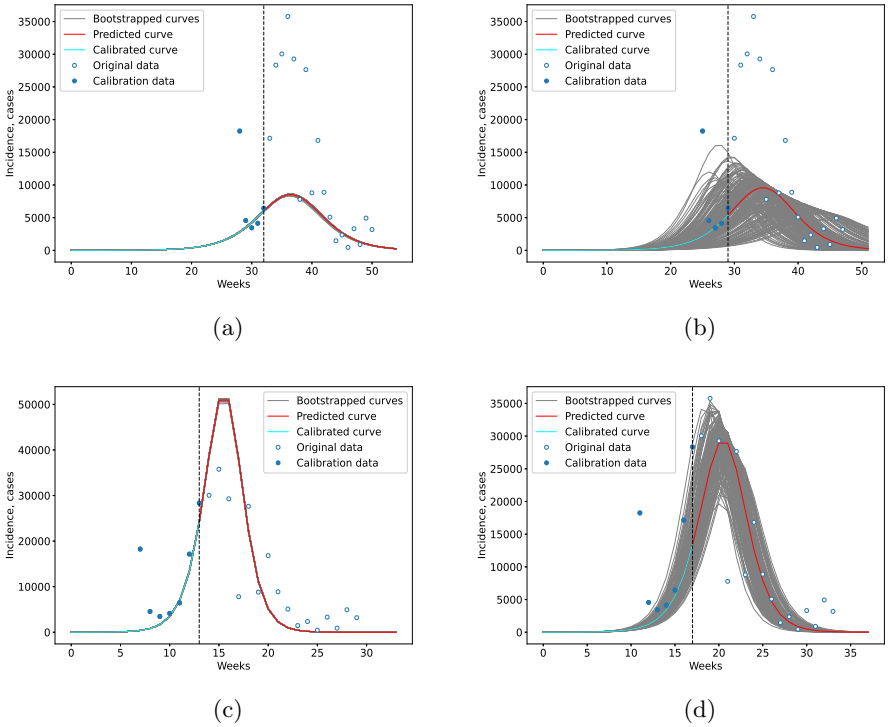


Fig. 6: Forecast visualization for the model calibrated on samples of 5 (a,b) and 7 (c,d) data points; gray curves represent the uncertainty in the forecast with Poisson (a,c) and negative binomial (b,d) error structures, cyan curve is the model best fit to the data sample, the red line is a prediction.

Table 3: The root mean squared errors of the forecasts

| Sample size | RMSE, Poisson | | RMSE, Negative binomial | |
|---|---|---|---|---|
| | Mean | 95% CI | Mean | 95% CI |
| 5 | 11823.2168 | (11819.3652, 11827.0683) | 13229.16249 | (13012.460, 13445.8649) |
| 6 | 9001.0666 | (8996.8640, 9005.2692) | 8529.351404 | (8369.3499, 8689.35282) |
| 7 | 9775.0136 | ( 9767.2357, 9782.7916) | 7564.4317 | (7459.4304, 7669.4331) |

ICCS Camera Ready Version 2023
To cite this paper please use the final published version:
DOI: 10.1007/978-3-031-36024-4_23

## 5 Conclusion

In this paper, we proposed an algorithm which is able to estimate parameter and forecasting uncertainty caused by the variance in the incidence data. For that purpose, by exploiting a framework for uncertainty estimation in epidemiological setting proposed by Chowell in [3], we have performed uncertainty quantification procedures and the interval prediction of disease incidence on the limited data points. In our case study, the confidence intervals obtained by assuming Poisson error structure are rather narrow if compared with variance in initial data, which raises some questions about the adequacy of this error structure. It is shown that negative binomial error structure is a better solution to account for observed overdispersion in the epidemic data. It is worth noting that the variance of this distribution was set somewhat arbitrarily based on few experiments. Ideally, the assessment of variance should be performed after extensive computational experiments, which will help establish the most adequate variance-to-mean ratio.

The presented uncertainty assessment methods and their planned development make it possible to give recommendations on what nomenclature and frequency of data collection related to the dynamics of acute respiratory viral infections is necessary and sufficient for retrospective analysis and forecasting of incidence with a given level of accuracy. Although so far we tested the described methods only on influenza outbreak data, they can be easily applied for analysing the outbreaks of other epidemic ARIs, such as COVID-19. After further testing and validating the modeling and forecasting framework described in the paper, we plan to adapt it for the use in real-time influenza and COVID-19 surveillance in Russian Federation.

## References

1. Burns, C., Wright, J., Pierson, J., et al.: Evaluating uncertainty to strengthen epidemiologic data for use in human health risk assessments. Environmental Health Perspectives **122**(11), 1160–1165 (2014)
2. Chowell, G., Ammon, C., Hengartner, N., Hyman, J.: Transmission dynamics of the great influenza pandemic of 1918 in Geneva, Switzerland: Assessing the effects of hypothetical interventions. Journal of Theoretical Biology **241**, 193–204 (2006)
3. Chowell, G.: Fitting dynamic models to epidemic outbreaks with quantified uncertainty: A primer for parameter uncertainty, identifiability, and forecasts. Infectious Disease Modelling **2**(3), 379–398 (2017)
4. Chowell, G., Luo, R.: Ensemble bootstrap methodology for forecasting dynamic growth processes using differential equations: application to epidemic outbreaks. BMC Medical Research Methodology **21** (2021)
5. Davison, A.C., Hinkley, D.V., Young, G.A.: Recent developments in bootstrap methodology. Statistical Science **18**, 141–157 (2003)
6. Efron, B., Tibshirani, R.: Bootstrap methods for standard errors, confidence intervals, and other measures of statistical accuracy. Statistical Science **1**, 54–75 (1986)
7. Hilbe, J.M.: Negative Binomial Regression Second Edition. Cambridge University Press (2011)

ICCS Camera Ready Version 2023
To cite this paper please use the final published version:
DOI: 10.1007/978-3-031-36024-4_23

8. Huaman, I., Plesovskaya, E.P., Leonenko, V.N.: Matching model complexity with data detail: influenza propagation modeling as a case study. 2022 IEEE International Multi-Conference on Engineering, Computer and Information Sciences (SIBIRCON) pp. 650–654 (2022)
9. Jurek, A., Maldonado, G., Greenland, S., et al.: Exposure-measurement error is frequently ignored when interpreting epidemiologic study results. European Journal of Epidemiology **21**, 871–876 (2006)
10. Kimab, D.R., Hwang, S.Y.: Forecasting evaluation via parametric bootstrap for threshold-INARCH models. Communications for Statistical Applications and Methods **27**, 177–187 (2020)
11. Krivorot'ko, O., Kabanikhin, S., Zyat'kov, N., et al.: Mathematical Modeling and Forecasting of COVID-19 in Moscow and Novosibirsk Region. Numerical Analysis and Applications **13**, 332–348 (2020)
12. Kulesa, A., Krzywinski, M., Blainey, P., Altman, N.: Sampling distributions and the bootstrap. Nature Methods **12**, 477–478 (2015)
13. Lee, V.J., Tok, M.Y., Chow, V.T., Phua, K.H., et al.: Economic analysis of pandemic influenza vaccination strategies in Singapore. PLOS One **4**(9), 1–8 (09 2009). https://doi.org/10.1371/journal.pone.0007108
14. Leonenko, V., Bobashev, G.: Analyzing influenza outbreaks in Russia using an age-structured dynamic transmission model. Epidemics **29** (2019)
15. Leonenko, V.N.: Herd immunity levels and multi-strain influenza epidemics in Russia: a modelling study. Russian Journal of Numerical Analysis and Mathematical Modelling **36**(5), 279–293 (2021)
16. Leonenko, V.N., Ivanov, S.V.: Fitting the SEIR model of seasonal influenza outbreak to the incidence data for Russian cities. Russian Journal of Numerical Analysis and Mathematical Modelling **26**, 267–279 (2016)
17. Leonenko, V.N., Ivanov, S.V.: Prediction of influenza peaks in Russian cities: Comparing the accuracy of two SEIR models. Mathematical Biosciences & Engineering **15**(1), 209 (2018)
18. Lloyd, A.: Sensitivity of model-based epidemiological parameter estimation to model assumptions. Mathematical and Statistical Estimation Approaches in Epidemiology. pp. 123—141 (2009)
19. López, M., Peinado, A., Ortiz, A.: Characterizing two outbreak waves of COVID-19 in Spain using phenomenological epidemic modelling. PLOS One **16** (2021)
20. Morillas, F., Valero, J.: Random resampling numerical simulations applied to a SEIR compartmental model. The European Physical Journal Plus **136** (2021)
21. Ning, X., Jia, L., et al.: Epi-DNNs: Epidemiological priors informed deep neural networks for modeling COVID-19 dynamics. Computers in Biology and Medicine (2023)
22. Puth, M., Neuhäuser, M., Ruxton, G.: On the variety of methods for calculating confidence intervals by bootstrapping. Journal of Animal Ecology **84**, 892–897 (2015)
23. Ranker, L., Petersen, J., Fox, M.: Awareness of and potential for dependent error in the observational epidemiologic literature: A review. Annals of Epidemiology **36**, 15–19 (2019)
24. Roosa, K., Chowell, G.: Assessing parameter identifiability in compartmental dynamic models using a computational approach: application to infectious disease transmission models. Theoretical Biology and Medical Modelling **16** (2019)
25. Roosa, K., Luo, R., Chowell, G.: Comparative assessment of parameter estimation methods in the presence of overdispersion: a simulation study. Mathematical Biosciences and Engineering **16**, 4299–4313 (2019)

ICCS Camera Ready Version 2023
To cite this paper please use the final published version:
DOI: 10.1007/978-3-031-36024-4_23

26. Samsuzzoha, M., Singh, M., Lucy, D.: Uncertainty and sensitivity analysis of the basic reproduction number of a vaccinated epidemic model of influenza. Applied Mathematical Modelling **37**(3), 903–915 (2013)
27. Swallow, B., Birrell, P., Blake, J., et al: Challenges in estimation, uncertainty quantification and elicitation for pandemic modelling. Epidemics **38** (2022)
28. Zelner, J., Riou, J., Etzioni, R., Gelman, A.: Accounting for uncertainty during a pandemic. Patterns **2**(8) (2021)

ICCS Camera Ready Version 2023
To cite this paper please use the final published version:
DOI: 10.1007/978-3-031-36024-4_23